Appl. Phys. B 83, 491–495 (2006)
DOI: 10.1007/s00340-006-2231-0

Applied Physics B
Lasers and Optics

T. OKSENHENDLER[1,✉]
D. KAPLAN[1]
P. TOURNOIS[1]
G.M. GREETHAM[2]
F. ESTABLE[2]

Intracavity acousto-optic programmable gain control for ultra-wide-band regenerative amplifiers

[1] Fastlite, Bât 403, Ecole Polytechnique, 91128 Palaiseau, France
[2] Amplitude Technologies, 2, rue du Bois Chaland, 91029 Evry, France

Received: 9 November 2005/Revised version: 16 February 2006
Published online: 5 May 2006 •

ABSTRACT We have developed a new Brewster-cut acousto-optic programmable gain control filter to optimize the spectral losses inside a regenerative cavity. This spectral amplitude control combined with an acousto-optic programmable dispersive filter for the spectral phase control optimizes, in a few steps of a direct algorithm, the performance of a 10-Hz CPA Ti:sapphire laser to 18-fs pulse duration, 1.2% RMS energy stability and 10^7 contrast ratio.

PACS 42.65.Re; 42.79.Jq

Chirped-pulse amplification (CPA) currently produces multiterawatt pulses of approximately 30-fs duration which are used for a variety of high-intensity ($> 10^{18}$ W/cm^2) and high-field applications such as the generation of ultra-fast soft or hard X-ray radiation [1], the generation of high-order harmonics [2] and the realization of table-top sources of high-energy electrons or protons [3]. Higher intensities can be reached by either increasing pulse energies or shortening pulse durations. The high cost of raising the pulse energy favors the shorter pulse duration approach.

Shorter pulse durations (sub-20 fs) in CPA lasers have been demonstrated by a reduction of gain narrowing in three ways:

1. Pre-compensation of the gain narrowing by the use of an acousto-optic programmable dispersive filter (AOPDF) before the amplifier [4].
2. Introduction of spectral filters, such as Fabry–Pérot etalons [5], birefringent filters, spatial masks in between Brewster prisms [6] or spectral loss managed multiple dielectric layers [7].
3. Wavelength-selective pumping of a multipass amplifier [8].

The AOPDF approach is limited because large enhancements of the bandwidth require strong reduction of the energy of the seed pulses. The drawbacks of the intracavity spectral filters are the lack of programmability and the generation of artifacts. The wavelength-selective pumping scheme adds complexity to the laser setup and may lead to significant spatial chirp requiring a multipass configuration and cryogenic cooling.

In this letter we report the development of a new intracavity acousto-optic programmable gain control filter (AOPGCF) for ultra-wide-band regenerative amplification. We have developed a new Brewster-cut acousto-optic collinear beam filter that accurately controls the spectral losses of a linear regenerative cavity. The spectral losses are introduced through partial diffraction of the unwanted spectral components. The spectral transmission of the filter is thus modified by the diffraction: total diffraction of a wavelength corresponds to zero transmission and no diffraction of a wavelength corresponds to total transmission of this wavelength. To optimize diffraction efficiency and spectral resolution, the AOPGCF is based on the same collinear beam interaction geometry as the AOPDF [9]. In this geometry, the incident, diffracted and acoustic beams are nearly collinear in energy directions leading to a long interaction length, i.e. a high diffraction efficiency and a high resolution. As the physical constants of the crystal used (TeO_2) are well known, the calibration is carried out by either an acoustic frequency tuning or a crystal tilt in the main interaction plane. Calibration accuracy is directly checked on the spectrum: complete diffraction of a narrow wavelength range generates a hole in the output spectrum; matching the measured wavelength of the hole and the wavelength programmed by the device control software allows one to calibrate the AOPGCF. The Brewster cut of optical faces avoids insertion losses and spurious pulse replicas.

The main drawback of this device is the dispersion of the 25-mm-long TeO_2 crystal (12 406 fs^2, 8114 fs^3, 4700 fs^4 at 800 nm for 25 mm), which is amplified by 24 passes through the crystal in the regenerative cavity. A simple tuning of the compressor allows compensation of the second order, but not for the huge third order ($\approx 200\,000$ fs^3) and higher-order terms. To optimally compress the pulse we have used a high-resolution

✉ Fax: +33-1-69-33-30-98, E-mail: thoksen@fastlite.com

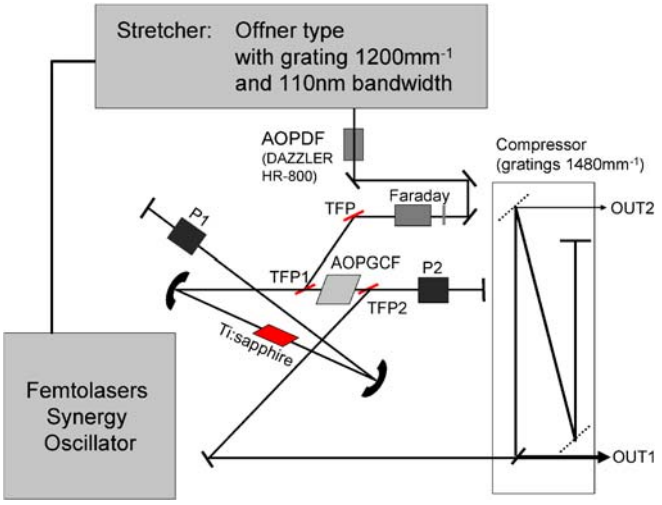

FIGURE 1 Schematic of the complete laser setup. TFP, thin-film polarizer; P, Pockels cell; AOPGCF, acousto-optic programmable gain control filter. The figure shows the seeding arrangement and the layout of the regenerative amplifier cavity containing the AOPGCF device. OUT1 is the output beam after pulse compression. OUT2 is the zero-order diffracted beam used for monitoring the spectrum for feedback control of the AOPGCF (see text)

AOPDF system (DAZZLER HR-800 from Fastlite).

The layout of the complete laser is shown in Fig. 1. The oscillator is an ultra-broad-band Femtolasers oscillator (> 100 nm FWHM) for good seeding over the complete bandwidth of the system. The stretcher is a conventional Offner-type stretcher with a 1200-lines/mm grating. The optical components limit the stretcher bandwidth to approximately 110 nm. At the output of the stretcher, we introduce the high-resolution AOPDF system (DAZZLER HR-800) to compensate for the phase over a temporal excursion of 8 ps. After the Faraday isolator, the AOPDF diffracted pulses are injected into the cavity through the thin-film polarizer TFP1. Pulsing the Pockels cell (P1) to its quarter-wave voltage traps a single pulse inside the cavity. At each round trip in the cavity, the pulse passes twice through the Ti:sapphire rod and the AOPGCF. The diffracted beam is lost and only the non-diffracted beam is amplified. The losses introduced by the AOPGCF are compensated by increasing the gain in the Ti:sapphire rod in order to keep the number of passes nearly constant. After approximately 24 passes (compared with ∼ 15 without the AOPGCF), the pulse is ejected from the cavity through the thin-film polarizer TFP2 by application of an electrical pulse to the second Pockels cell (P2). The output pulse is then re-compressed by a 1480-lines/mm grating compressor with a limited bandwidth of approximately 105 nm.

Many applications of sub-20-fs high-power laser systems require good stability and a high contrast ratio. We have characterized the spectrum, stability, contrast ratio and temporal intensity for each AOPGCF setup. The contrast ratio was measured by a high dynamic range third-order cross correlator (SEQUOIA from Amplitude Technologies) and the temporal intensity was measured by a Spectral Phase Interferometry for Direct Electric-field Reconstruction apparatus (SPIDER 20–80 fs from APE). The implementation of these diagnostics is sketched in Fig. 2. The spectrum is measured on the zero-order diffraction of the first compressor grating, which is also used to feed back to the AOPGCF for the control of the spectral amplitude. The pulse energy stability and temporal intensities are measured on the compressed pulse. In every experiment, the measured spectral phase is fed back to the AOPDF to flatten the phase [10]. The contrast measurement by a high dynamic range third-order cross correlator is of prime interest because of known spurious pulse apparitions in the former techniques using Fabry–Pérot etalons or birefringent filters and the importance of a good amplified spontaneous emission (ASE) contrast ratio for such high-power lasers. The pulse energy stability is measured by a photodiode and an oscilloscope.

The free-running spectrum of the laser, without an AOPGCF inside the cavity and with only AOPDF phase modulation, is measured to be 33 nm at full width at half maximum (FWHM), with pulse duration 29 fs FWHM, contrast ratio about 10^7 and pulse energy

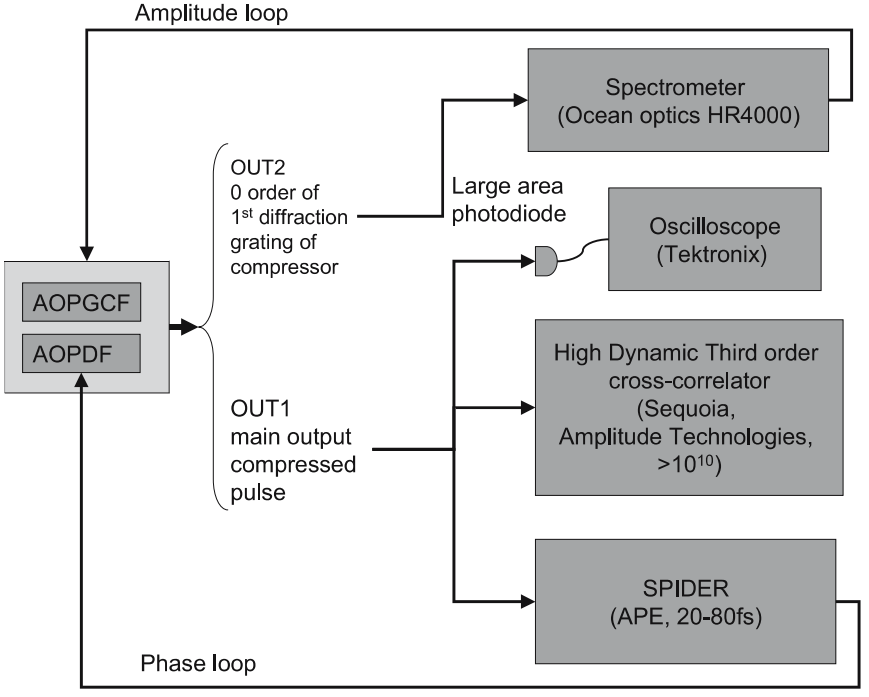

FIGURE 2 Schematic of the diagnostics setup with spectral amplitude and phase optimization loops

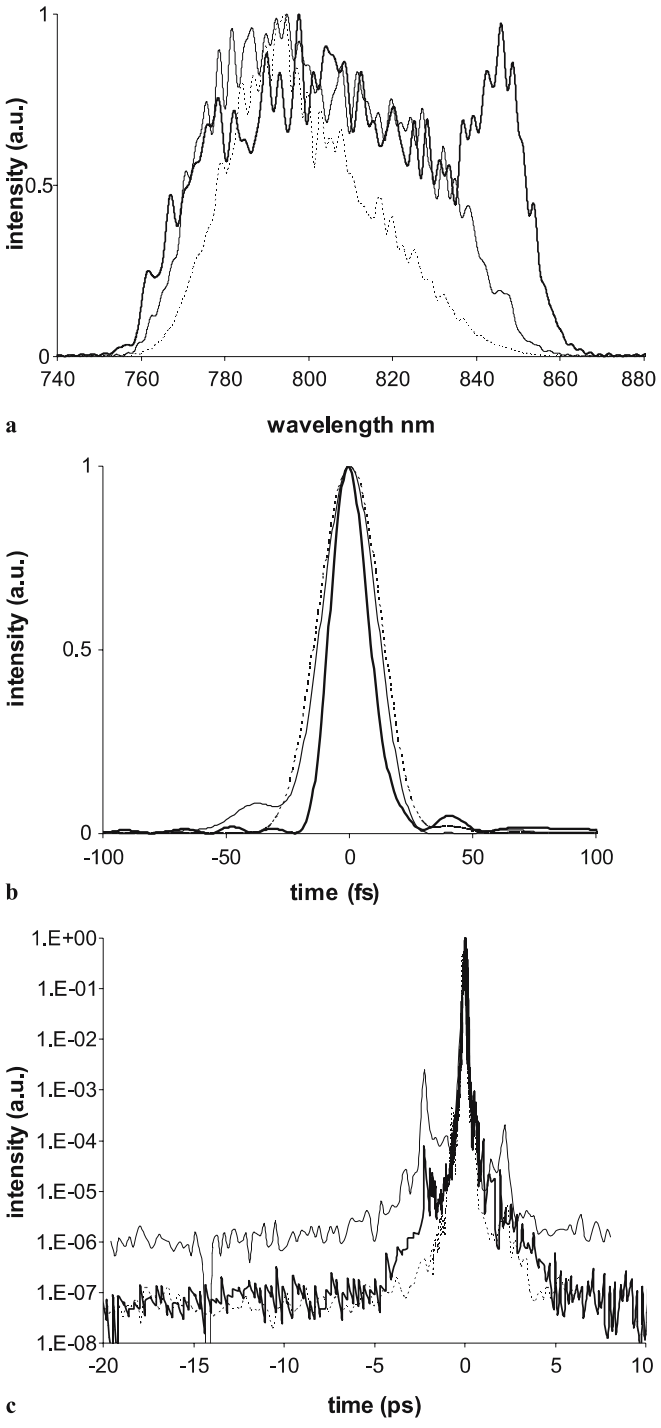

FIGURE 3 (**a**) Spectra, (**b**) temporal intensities and (**c**) high dynamic range third-order cross-correlator measurements for free-running system with AOPDF phase modulation only (*dotted curve*, 33 nm FWHM), with AOPDF amplitude and phase modulation (*thin solid curve*, 65 nm FWHM) and with AOPGCF optimization (*thick solid curve*, 80 nm FWHM). The pre-pulse at around −1 ps is probably due to Pockels cell misalignment and does not depend upon the AOPDF and AOPGCF setups

stability 2.6% root-mean square (RMS) (Fig. 3). Optimization of the bandwidth to 65 nm FWHM and the compressed pulse duration to 26.2 fs FWHM by AOPDF amplitude and phase modulation of the seed pulse degraded the contrast ratio to about 10^6 and the stability to 7.5% RMS. The deteriorations of the contrast ratio and the stability are due to the significant decrease in the seed pulse energy introduced by the AOPDF amplitude modulation. The small change in the pulse duration compared to the spectrum enlargement is due to the spectral amplitude shape modification from a Gaussian to a square shape. Fourier transforms of these spectra with flat phase lead to 28.5 fs for AOPDF phase modulation only and 24.3 fs for AOPDF phase and amplitude modulation.

The minimization of the laser pulse duration using the AOPGCF for spectral amplitude and the AOPDF for spectral phase optimizations necessitates only simple, direct, few-steps algorithms. Blind algorithm optimizations are not needed for spectral amplitude or phase optimizations.

The amplitude optimization is obtained by the direct feedback of the spectrum to the AOPGCF. The spectral amplitude of the output pulse is used directly as the spectral amplitude to be diffracted by the AOPGCF. Thus, the peaks are more attenuated and the spectrum converges onto a square shape. In fact, our goal is to determine the spectral losses that completely flatten the global gain of the amplifier. For 100-nm bandwidth, this process needs only a few steps (< 20). The final spectral losses thus determined can be used as long as the cavity does not change. Day to day fluctuations are small enough not to require major re-optimization. With the spectral losses determined, the amplifier acts as a flat-gain amplifier except for its saturation. An arbitrary spectral amplitude shape can then be obtained through four or five steps of spectral amplitude shaping with the AOPDF. All these optimizations were semi-automatically done in this experiment, necessitating approval of the end user. Complete automation of the optimization should lead to a less than a minute optimization process on a 10-Hz laser.

The flat phase optimization was simply obtained by introducing in the AOPDF the opposite of the phase measured by the SPIDER. For very large phase variations, more than one optimization loop was necessary.

The key point of these two optimizations is the calibration of the control systems (AOPDF and AOPGCF) with the measurement devices (SPIDER and spectrometer).

The bandwidth is limited by the compressor grating size to 105 nm. Thus, the best result we obtain is close to this bandwidth (80 nm FWHM). The 500-μJ pulse is sub-20 fs (18 fs FWHM) in duration and clean on its leading

edge; the contrast ratio is as good as without regenerative pulse shaping (10^7) and the energy stability better (1.2% RMS).

Theoretically, we expect these results because the ASE contrast ratio depends principally upon the seeding energy [11] and the stability of the laser could be largely improved by fine tuning of the global cavity losses [12]. The seeding energy is not decreased when using the AOPGCF because gain narrowing is compensated on each pass, unlike an AOPDF gain narrowing compensation where the seed pulse is subject to large amplitude modulation. The improvement of the pulse energy stability by a factor of two is obtained as the global loss tuning by the AOPGCF enables optimum saturation of the cavity for stabilization to be reached. This stability should be improved even further, but we have not optimized the global losses for this purpose.

The output pulse energy was limited to about 500 μJ to avoid any damage in the AOPGCF crystal. A higher energy level necessitates a larger spot size in the crystal, decreasing the simplicity and stability of the cavity. Joule-level pulses should be possible by post-amplification through a multipass amplifier. Gain narrowing is then pre-compensated by amplitude shaping of the 500-μJ pulse. The stability improvement will not be kept through post-amplification, but the contrast ratio should not degrade as it is mostly due to the first amplifier seeding energy. Pre-compensation of the gain narrowing on the scale of four orders of magnitude amplification (from 500 μJ to 5 J) should not affect the ASE contrast ratio.

In conclusion, we have developed a new intracavity acousto-optic programmable gain control filter (AOPGCF). We have demonstrated a broad amplified spectrum of 500-μJ, sub-20-fs optical pulses without contrast degradation and with stability enhancement. Even shorter pulses around 15 fs should be obtained by changing bandwidth-limiting optical components (Faraday isolator, gratings, mirrors, etc.). The device is fully software controlled and optimization of the laser bandwidth is completely done by software. Complete automation of the optimization is possible and requires only a few steps (< 30). The flexibility makes possible any kind of amplitude shaping, including two-color femtosecond pulses.

REFERENCES

1 A. Rousse, K. Ta Phuoc, R. Shah, A. Pukhov, E. Lefebvre, V. Malka, S. Kiselev, F. Burgy, J.-P. Rousseau, D. Umstadter, D. Hulin, Phys. Rev. Lett. **93**, 135 005 (2004)
2 D.H. Reitze, S. Kazamias, F. Weihe, G. Mullot, D. Douillet, F. Augé, O. Albert, V. Ramathanan, J.-P. Chambaret, D. Hulin, P. Balcou, Opt. Lett. **29**, 86 (2004)
3 V. Malka, S. Fritzler, E. Lefebvre, M.-M. Aleonard, F. Burgy, J.-P. Chambaret, J.-F. Chemin, K. Krushelnick, G. Malka, S.P.D. Mangles, Z. Najmudin, M. Pittman, J.-P. Rousseau, J.-N. Scheurer, B. Walton, A.E. Dangor, Science **298**, 22 (2002)
4 F. Verluise, V. Laude, Z. Cheng, C. Spielmann, P. Tournois, Opt. Lett. **25**, 575 (2000)
5 C.P.J. Barty, T. Guo, C. Le Blanc, F. Raksi, C. Rose-Petruck, J. Squier, K.R. Wilson, V.V. Yakovlev, K. Yamakawa, Opt. Lett. **21**, 668 (1996)
6 C.P.J. Barty, G. Korn, F. Raksi, C. Rose-Petruck, J. Squier, A.-C. Tien, K.R. Wilson, V.V. Yakovlev, K. Yamakawa, Opt. Lett. **21**, 219 (1996)
7 H. Takada, M. Kakehata, K. Torizuka, Jpn. J. Appl. Phys. **43**, 1485 (2004)
8 C.P. Hauri, M. Bruck, W. Kornelis, J. Biegert, U. Keller, Opt. Lett. **29**, 201 (2004)
9 D. Kaplan, P. Tournois, J. Phys. IV France **12**, 69 (2002)
10 T. Oksenhendler, P. Rousseau, R. Herzog, O. Gobert, M. Perdrix, P. Meynadier, in *CLEO 2000*, CThM44
11 V.V. Ivanov, A. Maksimchuk, G. Mourou, Appl. Opt. **42**, 7231 (2003)
12 F.P. Strohkendl, D.J. Files, L.R. Dalton, J. Opt. Soc. Am. B **11**, 742 (1994)